Distribution of Actual Evapotranspiration over Yinchuan Plain, an Arid Area in China

Xiaomei Jin (1), Renhong Guo (1), Zoltan Vekerdy (2)

(1) School of Water Resources and Environment, China University of Geosciences, Beijing, 100083, China;

(2) Faculty of ITC, University of Twente, Enschede, 7500AE,Netherlands;

(1)jinxm@cugb.edu.cn; grenhong@163.com; (2)z.vekerdy@utwente.nl

Abstract: Evapotranspiration (ET) is a major loss flux of the water balance in arid and semi-arid areas. The estimation of actual evapotranspiration in regional scale has significance for environmental and hydrological purposes. Spatial distribution of evapotranspiration and its relationship with vegetation, water table depth in the arid Yinchuan plain of China was studied by combining remote sensing data with groundwater depth observation. The vegetation cover was quantified with the NDVI, ET was estimated with the Surface Energy Balance System (SEBS), and the water table depths were measured in monitoring wells. There were 3 cloud-free and atmospherically corrected MODIS satellite images in July 2004 used in the SEBS algorithm to determine the actural evapotranspiration. 520 groundwater observations in the same season were applied to analyze the relationship between evapotranspiration and water table depth. The result showed that the evaporation from the farmland is at the value of 3.9 mm per day and the minimum value of 2 mm is for the bare soil. The evapotranspiration of shrub and grassland is in average value of 2.5 mm per day and 3.2 mm is for the farmland in the plain. The plain is covered by vegetation when the NDVI of the area is larger than 0.2 and that water table depth is an important factor influencing the ET in the arid region: the deeper the groundwater, the less the ET. The threshold depth of groundwater evaporation is 6 m with vegetation cover in raining season.

Keywords: evapotranspiration; SEBS; water table depth; NDVI; Yinchuan Plain

1. Introduction

Evapotranspiration (ET) is the main part of water balance and plays an important role in the hydrological process. The surface ET on a regional scale can substantially influence the amount and spatial distribution of water resources. In an arid inland basin, ET is the major loss variable in water budget. It varies with land surface and local meteorological conditions, and it is difficult to be quantified (Sun et al. 2004). Therefore, quantitative estimation of surface ET is essential for understanding the hydrological cycle, water management, and sustainable utilization of water resources (Glenn et al. 2007; Yang et al. 2010; Rwasoka et al. 2011; Nagler et al. 2013).

Yinchuan Plain is an inland basin rich in mineral resources in northwestern China. However, the plain is a water shortage area due to a dry climate and fast economic development. Sustainable development of Yinchuan Plain will mostly depend on the efficient utilization and strict management of water resources, which require a relatively accurate estimation of ET on a regional scale.

As one of the least-satisfactorily explained components of the water cycle, the ET cannot be measured directly but can be estimated by mass transfer or energy (Kite 2000). Remote sensing is an efficient tool to obtain the spatial and temporal variability of the ground surface over large areas. The ET estimation based on remote sensing techniques has developed rapidly since thermal infrared data was first used for evapotranspiration prediction (Brown et al. 1973). With the advantage of frequent updates and large area coverage, the remote sensing data has been used for ET estimation in many approaches (Kite and Pietroniro 1996; Rango and Shalaby 1999; Sobrino et al. 2007). The satellite images can provide regional scale land surface information effectively and can be used to estimate ET through a remote sensing method without quantifying other hydrological parameters (Morse et al. 2000). Since ET cannot be measured directly by remote sensing, some models of indirect estimation of ET have been proposed for quantifying the energy balance parameters such as net radiation, soil heat flux, sensible heat flux, and then ET estimation (Menenti and Choudhury 1993; Norman et al, 1995; Roerink et al. 2000; Bastiannssen et al. 2002; Su 2002). Based on Gowda *et al.* and Kalma *et al.*, the evapotranspiration estimation models using satellite data can be divided into two classes:

(1) Semi-physical or physical approaches; (2) Empirical relationships for estimation of evapotranspiration. As Kustas and Anderson stated, the physically based surface energy balance (SEB) models, especially SEBS, are less site-specific and require little subjective intervention, as opposed to techniques requiring the selection of hot and cold endpoints in the scene (Su 2002; Bastiaanssen et al. 1998; Allen et al. 2007). Sun *et al.* further put forward a simplified land surface model to calculate ET using the parameters estimated by a new stationarity-based method which couples the energy

balance and water. The parameter estimated by the stationarity-based method can avoid calibration with field observation ET and can be applied broadly in a harsh area which has no continuous forcing (precipitation and radiation) and surface states (soil moisture and temperature). These physical models can also be served as a useful tool when time series of evapotranspiration is needed.

Physically based SEB models can be divided into single-source (e.g., SEBS, SEBAL) and two-source (e.g., TSEB) bulk transfer equations for sensible heat flux estimation (Su 2002; Kustas & Norman 1997). Many studies have indicated that both single-source and two-source models can provide good results for the surface energy balance partitioning at different scales (Anderson et al. 2007; Su et al. 2001; Melesse & Nangia. 2005). The single-source models were used relatively widely in hydro-meteorological fields due to their simplicity. For example, the SEBAL model can estimate actual ET by computing the different variables of the energy balance of the land surface (Melesse et al. 2006; Senay et al. 2007; Melesse et al. 2008). The modified single-source models such as SEBS can adjust the differences between aerodynamic and radiometric surface temperatures in partial vegetation cover by employing physical models of soil–canopy heat exchange instead of separation of canopy and soil as two source terms (Kustas et al. 2007). Further, the modified surface energy budget technique can also be applied to map the distribution of lake evaporation and wetland ET (Melesse et al. 2009).

The final aim of deriving the evapotranspiration by remote sensing is to reach good operational application under different land cover conditions (Jia et al. 2003; Gokmen et al. 2012). The SEBS model has been validated in operational utility of evapotranspiration deriving for sparsely vegetated and dry areas (Ma et al. 2007; Jin et al. 2009), and thus it was selected as the main method for regional evapotranspiration estimation in this study.

The main objective of this study is to estimate the ET of the Yinchuan Plain and to discuss its controlling factors. The specific objectives are: (1) to estimate the ET_a of the Yinchuan Plain using MODIS land products; (2) to discuss the controlling factors of regional ET_a, such as climate factors, vegetation, land cover types, and water table depth.

2. Study Area

The study area is the Yinchuan Plain which is located in the upstream area if the Yellow river between the Helan mountain and the Erdos plateau (105°45′- 106°56′E and 37°46′-39°23′N) in northwestern China. The plain has a total area of 7790 km2 and is an important industrial and agricultural region in the Yellow River basin and a core area of economic development in Ningxia Autonomous Region. Fast development of the region's economy in recent years has resulted in overuse of groundwater resources and caused the decline of groundwater levels in the regional aquifers.

The surface elevation of the Yinchuan Plain decreases gradually from south to north and varies between 1100 m and 1500 m. With a typical continental and temperate arid climate, the precipitation in the study area is relatively small and concentrated in summer months from June to September. The mean annual precipitation is 185 mm, whereas the annual evaporation is 1825 mm, about 10 times of the annual precipitation. The Yellow River, the largest and longest river in the study area, flows from sourth to north through the plain (Figure 1).

The vegetation cover in the region varies spatially and changes with time, and was quantified with the Normalized Difference Vegetation Index (NDVI). The NDVI is an index derived from reflectance measurements in the red and infrared portions of the electromagnetic spectrum to describe the relative amount of green biomass present (Deering 1978). Higher NDVI values imply more vegetation coverage, lower values imply less vegetated coverage and zero indicates bare rock or a water body.

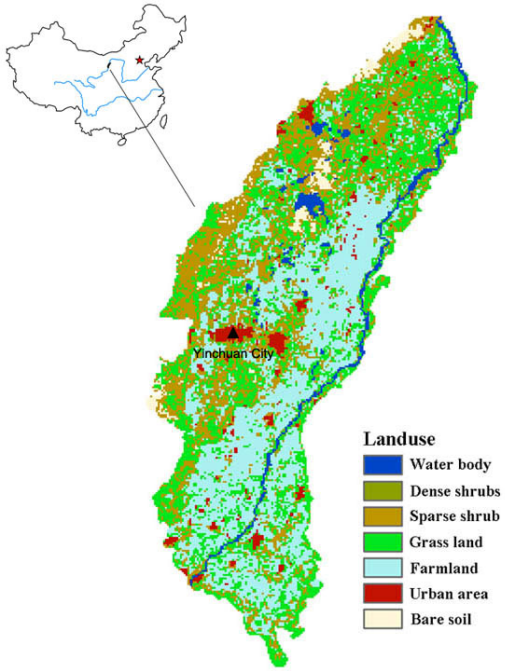

Figure 1 The landuse map of the Yinchuan Plain and its location in China.

3. Material and Methods

3.1. Surface Energy Balance System Algorithm

The SEBS algorithm, developed by Su (Su 2002), can be used to determine turbulent heat fluxes by employing satellite and meteorological data. It consists of: (1) an estimation of a series of land surface physical parameters, such as emissivity, albedo, vegetation coverage *etc.* based on spectral reflectance and radiance (Su et al. 1999); (2) an extended model of roughness length estimation for heat transfer (Su et al. 2001); (3) an

evaporative fraction estimation at limiting cases by energy balance. Three parts of information are required to be input in SEBS model. The first part is the land surface physical parameters, such as emissivity, albedo, temperature, vegetation coverage fraction, leaf area index and roughness height. The second part consists of climate factors of air temperature, air pressure, relative humidity and wind speed. The third part includes measured downward solar radiation and downward longwave radiation.

The basic surface energy balance equation can be expressed as:

$$R_n = G_0 + H + LE \quad (1)$$

where R_n is the net radiation, G_0 is the soil heat flux, H is the turbulent sensible heat flux, and LE is the turbulent latent heat. Net radiation, R_n, can be calculated by:

$$R_n = (1-\alpha)R_{swd} + \varepsilon R_{lwd} - \varepsilon\sigma T_0^4 \quad (2)$$

where α is the albedo, R_{swd} and R_{lwd} are the downward shortwave and longwave solar radiation (W m^{-2}), respectively, ε is the surface emissivity, σ is the Stefan–Bolzmann constant (5.67 ×10^{-8} W m^{-2} K^{-4}), and T_0 is the surface temperature (K). R_{swd} and R_{lwd} are estimated by meteorological measurement. α, ε and T_0 are physical parameters and can be obtained from remote sensing data.

The soil heat flux, G_0, which is energy entering into the soil, can be estimated as follows:

$$G_0 = R_n(\Gamma_c + (1-f_c)(\Gamma_s - \Gamma_c)) \quad (3)$$

where Γ_c and Γ_s are empirical coefficients. Γ_s is 0.315 for most bare soil condition (Kustas & Daughtry 1989) and Γ_c is commonly taken as 0.05 for full vegetation (Monteith 1973). The fractional canopy coverage f_c would be used as an interpolation between these cases and it can be determined by the scaled Normalized Difference Vegetation Index (NDVI) as:

$$f_c = \frac{NDVI - NDVI_{min}}{NDVI_{max} - NDVI_{min}} \quad (4)$$

where $NDVI_{max}$ and $NDVI_{min}$ are the NDVI for full vegetation (f_c = 1) and bare soil (f_c = 0), respectively.

In SEBS algorithm, the energy balance computation at limiting conditions would be used in order to derive the relative evaporation. At the dry limit, the sensible heat flux is at the maximum value, as well as evaporation would be zero because of limitation of soil moisture. The expression follows as:

$$H_{dry} = R_n - G_0 \quad (5)$$

At the wet limit, the sensible heat flux can be taken as the minimum value, and the ET is determined by the available energy in the given surface and the atmospheric conditions. It follows from the equation as:

$$H_{wet} = R_n - G_0 - LE_{wet} \quad (6)$$

Based on above process, the relative evaporation can be derived as:

$$\Lambda_r = 1 - \frac{H - H_{wet}}{H_{dry} - H_{wet}} \quad (7)$$

Finally, the evaporation fraction which is the energy used for the evapotranspiration process is estimated as:

$$\Lambda = \frac{LE}{H + LE} = \frac{LE}{R_n - G_0} = \frac{\Lambda_r LE_{wet}}{R_n - G_0} \quad (8)$$

The basic formulation of SEBS algorithm is constituted by Equation (1–8) (Su 2002). The daily evaporation can be estimated based on the assumption that evaporative fraction is approximately equal to the instantaneous value.

$$E_{daily} = 8.64 \times 10^7 \times \frac{\Lambda \overline{R_n}}{L\,\rho_w} \quad (9)$$

where E_{daily} is the actual evaporation (mm d^{-1}), L is the latent heat of vaporization (J kg^{-1}), $\overline{R_n}$ is the daily net radiation and is ρ_w the water density (kg m^{-3}).

Roughness terms are used to characterize the land surface condition. Roughness height of heat transfer, z_{oh}, can be estimated from a model by Su *et al.*. kB^{-1} or excess resistance term is taken into account to determine momentum and heat transfer over different ground surfaces in one source model of SEBS (Kwast et al. 2009). kB^{-1} is derived by:

$$kB^{-1} = \frac{kC_d}{4C_t \frac{u_*}{u(h)}\left(1-e^{-\frac{n_{ec}}{2}}\right)} f_c^2 + 2f_c f_s \frac{k.\frac{u_*}{u(h)}.\frac{z_{om}}{h}}{C_t^*} + kB_s^{-1} f_s^2 \quad (10)$$

where f_c is the fractional canopy coverage and f_s is fraction of non-vegetated soil (1- f_c). C_d is the drag coefficient of the foliage elements assumed to take the value of 0.2. C_t and C_t^* are coefficients of heat transfer for a leaf and soil, respectively. n_{ec} is the within-canopy wind speed profile extinction coefficient. z_{om} is the roughness length for momentum transfer. The term of kB_s^{-1} is used for bare soils and was formulated by Brutsaert (Brutsaert 1982). The roughness height, z_{oh} is determined from:

$$z_{oh} = \left(\frac{z_{om}}{exp(kB^{-1})}\right) \quad (11)$$

3.2. Dataset

The NDVI product from the Moderate Resolution Imaging Spectroradiometer (MODIS) of NASA's Earth Observing System was used in this research. The MODIS NDVI dataset (MOD 13 product) is based on 16-day composites and its spatial resolution is 250 m. These vegetation index maps have been corrected for molecular scattering, ozone and aerosol absorption. Currently, the MODIS NDVI product has been used throughout a wide range of disciplines, such as inter- and intra-annual global vegetation monitoring, climate and hydrologic modeling, agricultural activities and drought studies (Knight et al. 2006; Lunetta et al. 2006; Jin and Sader 2005; Sakamoto et al. 2005; Zhan et al. 2000). To be consistent with the groundwater data, the MODIS NDVI values of July 2004 were used to analyze the relationship between ET and vegetation in this study.

1-7 bands of the MODIS Surface-Reflectance Product (MOD 09) and 31, 32 bands of MODIS land surface temperature data (MOD 11) were selected which are based on 8-day composites and have spatial resolution of 500 m and 1000 m, respectively. 39 cloud-free MODIS images covered the Yinchuan Plain during April to October in 2004 were used to derive the evapotranspiration in large scale. In order to be consistent, the product of MOD 11 was resampled into the same spatial resolution of 500 m as MOD 9 and these two products of 2004 were used in SEBS in this study to estimate daily evaporation.

A total of 520 groundwater observation wells in the Yinchuan Plain were measured in July of 2004. The values of the groundwater depth were interpolated using Kriging with the same spatial resolution of 500 m × 500 m as the MODIS data (Figure 2). 27,540 pairs of the groundwater depth and evaporation estimated with the SEBS were obtained in the study area. The evaporation values corresponding to the same groundwater depth are averaged over the interval of 0.2 m so that the quantitative relationship between the averaged evaporation and the corresponding groundwater depth in the area can be established. The meteorological data used in this study includes sea level pressure, air temperature, wind speed, wind direction, relative humidity and pan evaporation (open water surface evaporation). Pre-processing of the data was done to derive the variables at satellite passing time needed as inputs for SEBS.

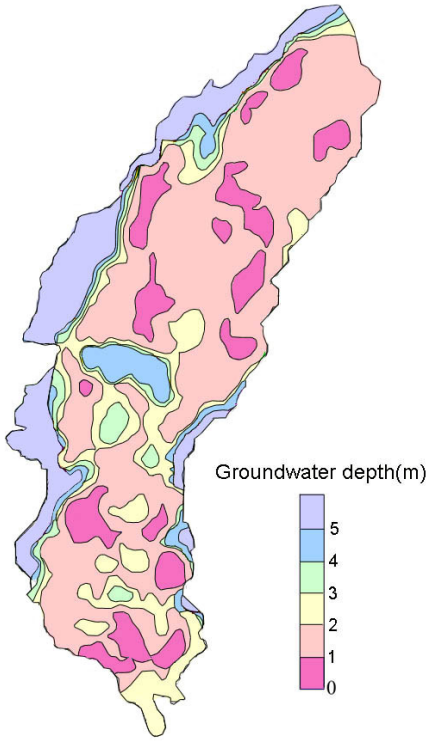

Figure 2 Contour map of water table depth in the Yinchuan plain in July of 2004 interpolated from the observed values.

4. Results

4.1. Spatial Distribution of Actual Evapotranspiration by SEBS

The results of average actual evapotranspiraiton from SEBS in July 2004 was showed in Figure 3. The irrigated farmland had relatively higher ET values of 3.9 mm.d^{-1}. The shrubs ET varied between 2.5 and3.2 mm.d^{-1} as the vegetation cover increases. The minimum ET estimates was 2 mm.d^{-1} for bare soil.

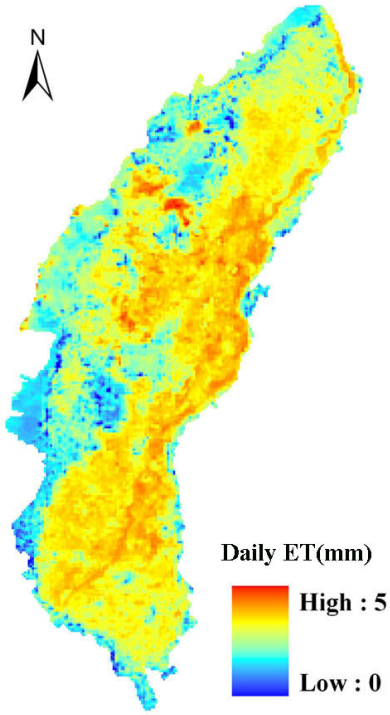

Figure 3 Spatial distribution of evapotranspiration of July 2004 in the Yinchuan Plain.

The land cover in the Yinchuan Plain in July was counted with MODIS satellite data (Figure 1). 37% of the plain was covered by cropland and 53% of the area was grassland and shrub. 4% of the plain was occupied by water body and 6% of the area was mixed urban area and bare soil. The variation of SEBS ET in different landform was illustrated in Figure 4 by combination of ET value with plain landform in GIS. The evaporation of bare soil was in the minimum value of 2.4 mm.d^{-1}. The ET of grassland and shrub was in average value of 3.5 mm.d^{-1} and 3.9 mm.d^{-1} was for the farmland in the plain (Figure 4).

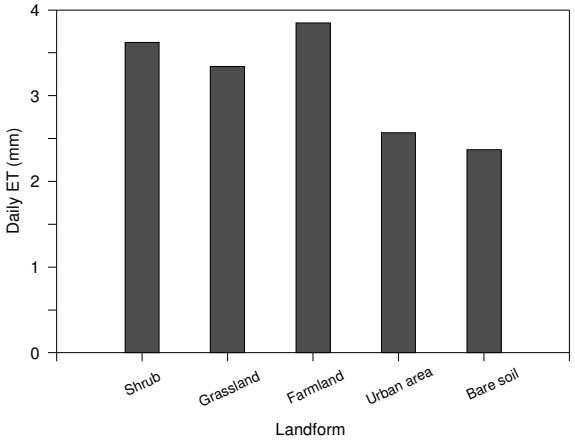

Figure 4 ET distribution of different landforms in the Yinchuan Plain.

4.2 Evapotranspiration and NDVI

MODIS NDVI data of July 2004 was used to analyze the distribution patterns of vegetation in the Yinchuan Plain and the image was selected for the same time of field survey on water table depth (Figure 5). No clouds disturbance was presented in the NDVI data.

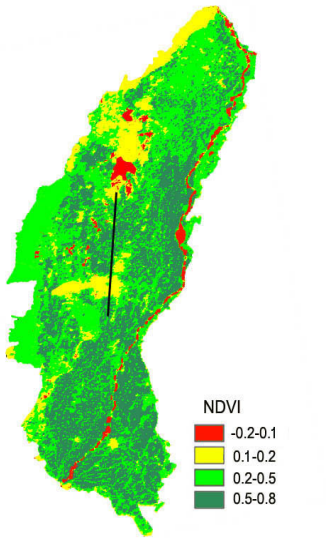

Figure 5 NDVI distribution of The Yinchuan Plain in July of 2004.

The relationship can be developed to relate NDVI and ET to vegetation cover using remote sensing data (Samani et al., 2011). For correlation analysis with ET, the NDVI map was upgraded to the same 500-m-resolution grid using the arithmetic mean. The new NDVI map matched the ET distribution map. For each grid cell, a pair of ET and NDVI can be read. There were in total 27540 pairs of ET and NDVI values. The NDVI values were grouped by 0.02 value ranges and the corresponding daily ET values were averaged. The relationship between the NDVI and daily ET obtained was presented as non-linear in Figure 6. The maximum daily ET of 5 mm was obtained at the NDVI value of -0.08. As the NDVI increases, ET decreases to its minimum of 2.4 mm at the NDVI value of 0.2. As the NDVI increased beyond 0.2, the ET increased to about 4 mm. This non-linear relationship can be explained as follows. A pixel becomes totally covered by water when the NDVI was smaller than 0 and ET (mainly evaporation from water surface) reaches its maximum value of 5 mm. As the NDVI increased from 0, the pixel was covered more and more by bare soil or urban area and reached minimum evaporation (2.4 mm) at NDVI = 0.2. As the NDVI increased beyond this point, the pixel was covered less and less by bare soil and more and more by vegetation and ET increases to about 4 mm at NDVI = 0.62 of farmland. Based on Figure 6, it can be deduced that there was vegetation on the ground when the NDVI was larger than 0.2. This result can be explained by the fact that vegetated area occupied 90% of the plain. The vegetation types in the plain can be divided into farmland, grass, dense shrub and sparse shrub. The area of sparse shrub was 155.75 km^2 and it was only occupied 2% of the total plain. The farmland, grass and dense shrub grow well in July and they had a relative high NDVI value and therefore NDVI = 0.2 was the threshold separating bare soil and vegetated area. NDVI is also a dominant impact factor for ET variation. Higher NDVI results in higher ET and they are highly positive correlated when the NDVI is largger than 0.2 in the Yinchuan Plain.

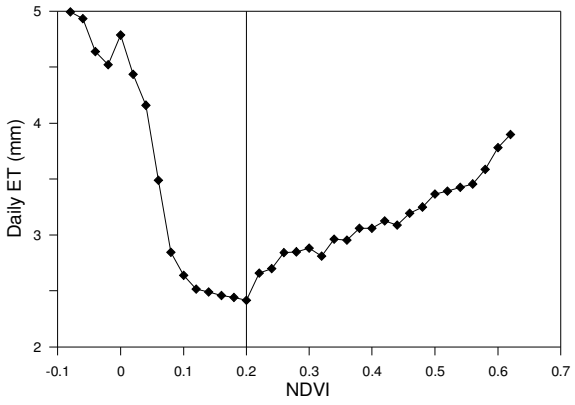

Figure 6 The relationship between the NDVI and daily ET in July of 2004.

Further validation analysis of NDVI in different landforms was presented in Figure 7. It can be noted that daily ET varied from 1.2 mm to 2.6 mm with NDVI ranged from 0.1 to 0.2. This result was then used in combination with relationship between ET and NDVI (Figure 6) to determine the threshold NDVI of bare soil. Figure 6 provided the same result of NDVI threshold for bare soil (Daily ET = 1.2 – 2.6 mm) as Figure 7 and it ranged from 0.1 to 0.2 in the Yinchuan Plain. On the other hand, the landuse map (Figure 1) and

NDVI distribution map (Figure 5) can also prove this supposition since the landuse map was validated by field work before.

Figure 7 NDVI of different landforms in a section of the Yinchuan Plain.

4.3 Evapotranspiration and Water table depth

The water table depth values were grouped by 0.2 m values ranges and the corresponding evapotranspiration values were averaged. The scatter plots evapotranspiration against water table depth were presented in Figure 8 and the black line refers to the variation of average daily evapotranspiration with water table depth. There is declining trend of daily evapotranspiration with increasing water table depth and the evapotranspiration stabilized at the value of 2.4 mm per day when the water table depth was deeper than 6 m. This phenomenon can be explained that in the areas of water table depth larger than 6 m, the recharge from groundwater was low and the surface evapotranspiration mainly come from precipitation and irrigation. On the other hand, the water loss of surface evapotranspiration was mainly recharged from groundwater and large part of surface evapotranspiration was groundwater evaporation when the groundwater depth was shallower than 6 m. Therefore, it is reasonable to think that the threshold depth of groundwater evaporation with vegetation cover of raining season in the Yinchuan plain was about 6 m. The groundwater evaporation was almost zero and surface evapotranspiration was roughly equal to soil water evaporation (2.4 mm) when the groundwater depth was larger than 6 m.

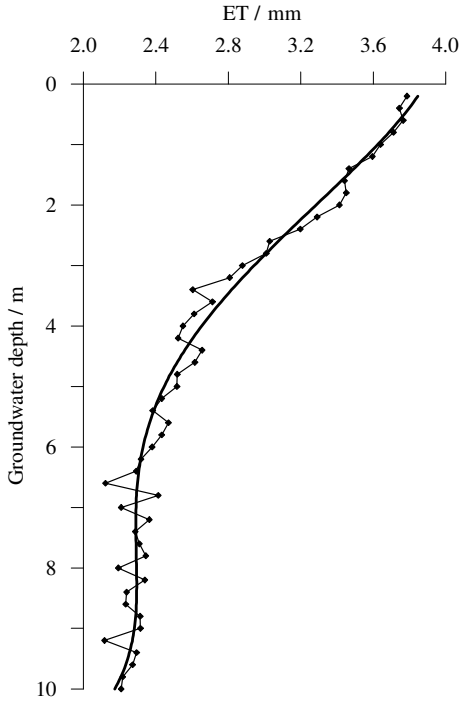

Figure 8 The relationship between daily evapotranspiration with water table depth in July.

5. Conclusions

The Surface Energy Balance System (SEBS) algorithm was used in this research to estimate spatial actual evapotranspiration in Yinchuan Plain. The impact of vegetation and water table depth in regional evapotranspiration was also investigated by combining remote sensing data with groundwater depth observations. The general conclusion of this study is that, groundwater depth is a key factor controlling the ET in an arid region: the deeper the groundwater, the less the ET on the ground. More specific conclusions are

1) The average daily evaporation of bare soil, shrub and grassland, farmland in the Yinchuan plain were at the value of 2.4 mm, 3.5 mm and 3.9 mm per day, respectively.

2) The reference value of NDVI threshold between bare soil and vegetation was 0.2 in the Yinchuan Plain.

3) Groundwater depth has influence on surface evapotranspiration in the plain. The ET decreased with groundwater depth and become stable (2.4 mm) when the water table depth was larger than 6 m. The threshold depth of groundwater evaporation of raining season in the Yinchuan Plain was about 6 m.

Overall, SEBS was proved to be a useful tool for estimation of actual evapotranspiration in regional area. The SEBS actual evapotranspiration can be very helpful for regional hydrological assessment, water resources management and planning in arid and semi-arid areas. However, the more incisive analysis of effect of water table depth on actual evapotranspiration is needed in the near future.

Acknowledgments

This study is supported by the European Union project IGIT titled as "Integrated geo-spatial information technology and its application to resource and environmental management towards the GEOSS" (grant agreement PIRSES-GA-2009-247608). The authors also would like to acknowledge the help of National Natural Science Foundation (41372250) and Fundamental Research Funds for the Central Universities granted by the Ministry of Education of China (2652014046).

References

1. Allen, R.G.; Tasumi, M.; Trezza, R. Satellite-based energy balance for mapping evapotranspiration with internalized calibration (METRIC)-Model. *J. Irrig. Drain. Eng.* **2007**, *133*, 380–394.
2. Anderson, M.C.; Kustas, W.P.; Norman, J.M. Upscaling flux observations from local to continental scales using thermal remote sensing. *Agron. J.* **2007**, *99*, 240–254.
3. Bastiaanssen, W.G.M.; Menenti, M.; Feddes, R.A.; Holtslag, A.A.M. A remote sensing surface energy balance algorithm for land (SEBAL). 1. Formulation. *J. Hydrol.* **1998**, *212–213*, 198–212.
4. Bastiaanssen, W.G.M.; Ahmed, M.; Chemin, Y. Satellite surveillance of evaporative depletion across the Indus Basin. *Water Resour. Res.* **2002**, *38*, 1273–1282.
5. Brown, K.W.; Rosenberg, N.J. A resistance model to predict evapotranspiration and its application to a sugar beet field. *Agron. J.* **1973**, *65*, 341–347.
6. Deering, D.W. Rangeland reflectance characteristics measured by aircraft and spacecraft sensor. Ph.D. Dissertation, Texas A&M University, College Station, **1978**, TX 38pp.
7. Glenn, E.P.; Huete, A.R.; Nagler, P.L.; Hirschboeck, K.K.; Brown, P. Review: Integrating remote sensing and ground methods to estimate evapotranspiration. *Crit. Rev. Plant Sci.* **2007**, *26*, 139–168.
8. Gokmen, M.; Vekerdy, Z.; Verhoef, A.; Verhoef, W.; Batelaan, O.; van der Tol, C. Integration of soil moisture in SEBS for improving evapotranspiration estimation under water stress conditions. *Remote Sens. Environ.* **2012**, *121*, 261–274.
9. Gowda, P.H.; Chavez, J.L.; Colaizzi, P.D.; Evett, S.R.; Howell, T.A.; Tolk, J.A. Remote sensing based energy balance algorithms for mapping ET. *Trans. ASABE* **2007**, *50*, 1639–1644.
10. Jia, L.; Su, Z.; van Den Hurk, B.J.J.M.; Menenti, M.; Moene, A.R.; de Bruin, H.A.R.; Yrisarry, J.J.B.; Ibanez, M.; Cuesta, A. Estimation of sensible heat flux using the surface energy balance system SEBS and ATSR measurements. *Phys. Chem. Earth* **2003**, *28*, 75–88.
11. Jin, S; Sader, S.A. MODIS time-series imagery for forest disturbance detection and quantification of patch size effects. *Remote Sens. Environ.* **2005**, *99*, 462–470.
12. Jin, X.M.; Schaepman, M.E.; Clevers, J.G.P.W.; Su, Z. Impact and consequences of evapotranspiration changes on water resources availability in the arid Zhangye Basin,China. *Int. J. Remote Sens.* **2009**, *30*, 3223–3238.
13. Kalma, J.D.; Mcvicar, T.R.; McCabe, M.F. Estimating land surface evaporation: A review of methods using remotely sensed surface temperature data. *Surv. Geophys.* **2008**, *29*, 421–469.
14. Kite, G.W.; Pietroniro, A. Remote sensing application in hydrological modeling. *Hydrol. Sci.* **1996**, *41*, 563–591.
15. Kite, G. Using a basin-scale hydrological mode to estimate crop transpiration and soil evaporation. *J. Hydrol.* **2000**, *229*, 59-69.
16. Knight, J.K.; Lunetta, R.L.; Ediriwickrema, J.; Khorram, S. Regional Scale Land-Cover Characterization using MODIS-NDVI 250m multi-temporal imagery: A phenology based approach. *GISci. Remote Sens.* **2006**, *43*, 1–23.
17. Kustas, W.P.; Daughtry, C.S.T. Estimation of the soil heat flux/net radiation ratio from spectral data. *Agricult. For. Meteorol.* **1989**, *49*, 205–223.
18. Kustas, W.P.; Norman, J.M. A two-source approach for estimating turbulent fluxes using multiple angle thermal infrared observations. *Water Resour. Res.* **1997**, *33*, 1495–1508.
19. Kustas, W.P.; Anderson, M.C.; Norman, J.M.; Li, F. Utility of radiometric—Aerodynamic temperature relations for heat flux estimation. *Bound.-Layer Meteorol.* **2007**, *122*, 167–187.
20. Lunetta, R.S.; Knight, J.F.; Ediriwickrema, J.; Lyon, J.G.; Worthy, L.D. Landcover change detection using multi-temporal MODIS NDVI data. *Remote Sens. Environ.* **2006**, *105*, 142–154.
21. Ma, Y.; Song, M.; Ishikawa, H.; Yang, K.; Koike, T.; Jia, L.; Menenti, M.; Su, Z. Estimation of the regional evaporative fraction over the Tibetan plateau area by using Landsat-7 ETM data and the field observations. *J. Meteorol. Soc. Jpn.* **2007**, *85A*, 295–309.
22. Melesse, A.M.; Nangia, V. Estimation of spatially distributed surface energy fluxes using remotely-sensed data for agricultural fields. *Hydrol. Process.* **2005**, *19*, 2653–2670.
23. Melesse, A.M.; Oberg, J.; Nangia, V.; Beeri, O.; Baumgartner, D. Spatiotemporal

dynamics of evapotranspiration at the Glacial Ridge prairie restoration in northwestern Minnesota. *Hydrol. Process.* **2006**, *20*, 1451–1464.
24. Melesse, A.M.; Frank, A.; Nangia, V.; Hanson, J. Analysis of energy fluxes and land surface parameters in a grassland ecosystem: A remote sensing perspective. *Int. J. Remote Sens.* **2008**, *29*, 3325–3341.
25. Melesse, A.M.; Abtew, W.; Dessalegne, T. Evaporation estimation of Rift Valley Lakes: Comparison of models. *Sensors* **2009**, *9*, 9603–9615.
26. Menenti, M.; Choudhury, B.J. Parametrization of Land Surface Evapotranspiration Using a Location Dependent Potential Evapotranspiration and Surface Temperature Range. In *Exchange Processes at the Land Surface for a Range of Space and Time Scales*; Bolle, H.J., Ed.; IAHS: Wallingford, USA, 1993; pp. 561–588.
27. Monteith, J.L. *Principles of Environmental Physics*; Edward Arnold: London, UK, 1973.
28. Morse, A.; Tasumi, M.; Allen, R.G.; Kramber, W.J. Application of the SEBAL Methodology for Estimating Consumptive Use of Water and Stream Flow Depletion in the Bear River Basin of Idaho through Remote Sensing. In *The Raytheon Systems Company-Earth Observation System Data and Information System Project*; Idaho, USA, 2000; pp. 107.
29. Nagler, P.L.; Glenn, E.P.; Nguyen, U.; Scott, R.L.; Doody, T. Estimation riparian and agricultural actual evapotranspiration by reference evapotranspiration and MODIS enhanced vegetation index. *Remote Sens.* **2013**, *5*, 3849–3871.
30. Norman, J.M.; Kustas, W.P.; Humes, K.S. A two-source approach for estimating soil and vegetation energy fluxes in observations of directional radiometric surface temperature. *Agricult. For. Meteorol.* **1995**, *77*, 263–293.
31. Rango, A.; Shalaby, A.I. Urgent Operational Applications of Remote Sensing in Hydrology. In *Operational Hydrology Report 43*; World Meteorology Organization: Geneva, Switzerland, 1999.
32. Roerink, G.J.; Su, Z.; Menenti, M. S-SEBI: A simple remote sensing algorithm to estimate the surface energy balance. *Phys. Chem. Earth B* **2000**, *25*, 147–157.
33. Rwasoka, D.T.; Gumindoga, W.; Gwenzi, J. Estimation of actual evapotranspiration using the surface Energy Balance System(SEBS) algorithm in the Upper Manyame catchment in Zimbabwe. *Phys. Chem. Earth* **2011**, *36*, 736–746.
34. Sakamoto, T.; Yokozawa, M.; Toritani, H.; Shibayama, M.; Ishitsuka, N.; Ohno, H. A crop phenology detection method using time-series MODIS data. *Remote Sens. Environ.* **2005**, *96*, 366–374.
35. Samani, Z.; Bawazir, S.; Skaggs, R.; Longworth, J.; Pinon, A.; Tran, V. A simple irrigation scheduling approach for pecans. *AGR. Water Manage.* **2011**, *98*, 661-664.
36. Senay, G.B.; Budde, M.; Verdin, J.P.; Melesse, A.M. A coupled remote sensing and simplified energy balance approach to estimate actual evapotranspiration from irrigated fields. *Sensors* **2007**, *7*, 979–1000.
37. Sobrino, J.A.; Gómez, M.; Jiménez-muñoz, J.C.; Olioso, A. Application of a simple algorithm to estimate daily evapotranspiration from NOAA-AVHRR images for the Iberian Peninsula. *Remote Sens. Environ.* **2007**, *110*, 139–148.
38. Su, Z.; Pelgrum, H.; Menenti, M. Aggregation effects of surface heterogeneity in land surface processes. *Hydrol. Earth Syst. Sci.* **1999**, *3*, 549–563.
39. Su, Z.; Schmugge, T.; Kustas, W.P.; Massman, W.J. An evaluation of two models for estimation of roughness height for heat transfer between the land surface and atmosphere. *J. Appl. Meteorol.* **2001**, *40*, 1933–1951.
40. Su, Z. The Surface Energy Balance System (SEBS) for estimation of turbulent heat fluxes. *Hydrol. Earth Syst. Sci.* **2002**, *6*, 85–99.
41. Sun, R.; Gao, X.; Liu, C.-M.; Li, X.-W. Evapotranspiration estimation in the Yellow River Basin, China using integrated NDVI data. *Int. J. Remote Sens.* **2004**, *10*, 2523–2534.
42. Yang, D.; Chen, H.; Lei, H. Estimation of evapotranspiration using a remote sensing model over agricultural land in the North China Plain. *Int. J. Remote Sens.* **2010**, *31*, 3783–3798.
43. Zhan, X.; Defries, R.; Townshend, J.R.G.; Dimiceli, C.; Hansen, M.; Huang, C.; Sohlberg, R. The 250m global land cover change product from the Moderate Resolution Imaging Spectroradiometer of NASA's Earth Observing System. *Int. J. Remote Sens*. **2000**, *21*, 1433-1460.

IGIT 2015

Tamás Jancsó – Péter Engler (eds)

Integrated geo-spatial information technology and its application to resource and environmental management towards GEOSS

2015

IGIT 2015 – International Conference

16- 17 January, 2015

Project No: 247608

Publisher: Nyugat-magyarországi Egyetem Kiadó, Sopron
ISBN 978-963-334-211-4